DEMETER satellite observations of lightning-induced electron precipitation

U. S. Inan,[1] D. Piddyachiy,[1] W. B. Peter,[1] J. A. Sauvaud,[2] and M. Parrot[3]

Received 2 January 2007; revised 21 February 2007; accepted 2 March 2007; published 5 April 2007.

[1] DEMETER spacecraft detects short bursts of lightning-induced electron precipitation (LEP) simultaneously with newly-injected upgoing whistlers, and sometimes also with once-reflected (from conjugate hemisphere) whistlers. For the first time causative lightning discharges are definitively geo-located for some LEP bursts aboard a satellite. The LEP bursts occur within <1 s of the causative lightning and consist of 100–300 keV electrons. First in-situ observations of large regions of enhanced background precipitation are presented. The regions are apparently produced and maintained by high rate of lightning within a localized thunderstorm. **Citation:** Inan, U. S., D. Piddyachiy, W. B. Peter, J. A. Sauvaud, and M. Parrot (2007), DEMETER satellite observations of lightning-induced electron precipitation, *Geophys. Res. Lett.*, *34*, L07103, doi:10.1029/2006GL029238.

1. Introduction

[2] Cyclotron-resonant loss of trapped electrons via scattering by lightning-generated whistler waves was indirectly evidenced as whistler-associated perturbations of subionospheric VLF signals [*Helliwell et al.*, 1973], and directly detected [*Voss et al.*, 1984] as LEP bursts (a multiplicity of successive pulses), in association with ducted whistlers. Based on interpretation [*Inan et al.*, 1985] of slow risetimes of VLF transmitter-induced precipitation pulses [*Imhof et al.*, 1983] multiple subsequent pulses were recognized to be due to atmospheric backscatter and mirroring [*Inan et al.*, 1989; *Voss et al.*, 1998].

[3] DEMETER observations constitute the first simultaneous in-situ detection of LEP bursts and whistler waves allowing direct comparison with theoretical model predictions (e.g., input wave power density versus resultant precipitation fluxes). Theoretical modeling indicates that LEP may be the dominant loss process at $L < 2.5$ [*Abel and Thorne*, 1998], and calibration of model results with DEMETER data can thus help better quantify the role of LEP in radiation belt loss. DEMETER data also provide us with the first evidence of large enhanced background LEP regions maintained by the high rate of flashes in a given thunderstorm.

[4] Detailed analysis [*Inan et al.*, 1989] revealed that (i) LEP flux-energy-time signature is consistent with pitch angle (α) scattering by whistlers, (ii) peak fluxes are small ($\sim 5 \times 10^3 - 10^5$ el/cm^2/s/sr), (iii) electrons are moved from just above the loss-cone edge to below it, with $\Delta\alpha_{max} < 1°$, and (iv) electrons precipitate at near-grazing angles, with substantial atmospheric backscatter [*Voss et al.*, 1998].

[5] In view of (iii) and (iv) electron detectors with typical large viewing angles (30° for DEMETER), either miss (viewing deep in the loss cone) newly scattered LEP electrons or observe them on top of large near loss-cone-edge flux (viewing vicinity of loss cone). LEP events may thus be more readily visible at European longitudes just east of the South Atlantic Anomaly (SAA), with the much lower background. In view of (ii) LEP bursts are not observable with most detectors with small (e.g., 0.01 cm^2 sr for NOAA POES) geometric factors designed for auroral fluxes.

[6] Ionospheric effects of LEP are observed (via subionospheric VLF) with steadily increasing accuracy and coverage, including identification of LEP due to nonducted whistlers [*Lauben et al.*, 2001, and references therein], precipitating electrons from large sectors (ground-footprints of 1000 km) of the radiation belts [*Clilverd et al.*, 2004; *Peter and Inan*, 2004], with many tens of LEP bursts per hour in localized thunderstorms [*Peter and Inan*, 2004].

2. Description of Experiment

[7] DEMETER is in a 700 km altitude 98.3° inclination orbit [*Parrot*, 2006]. We use data from the Electric Field

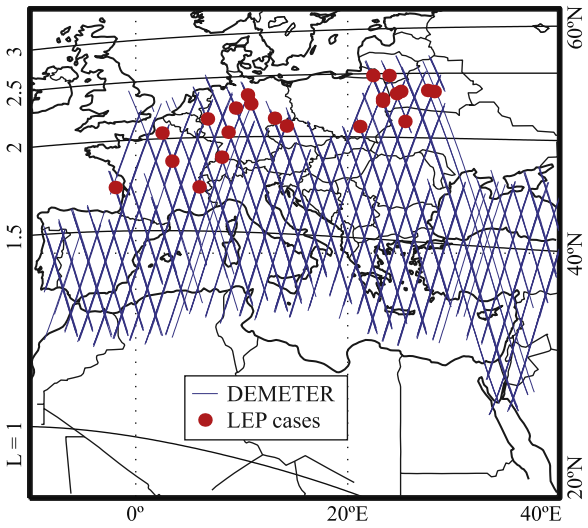

Figure 1. Ground-tracks (mapped along the field lines) of DEMETER passes for which burst mode data were available and analyzed. LEP events are shown by red dots. *L*-shell contours at ground level are shown for reference.

[1]Space, Telecommunications, and Radioscience Laboratory, Stanford University, Stanford, California, USA.
[2]Centre d'Etude Spatiale des Rayonnements, Centre National de la Recherche Scientifique, Toulouse, France.
[3]Laboratoire de Physique et Chimie de l'Environnement, Centre National de la Recherche Scientifique, Orléans, France.

0094-8276/07/2006GL029238$05.00

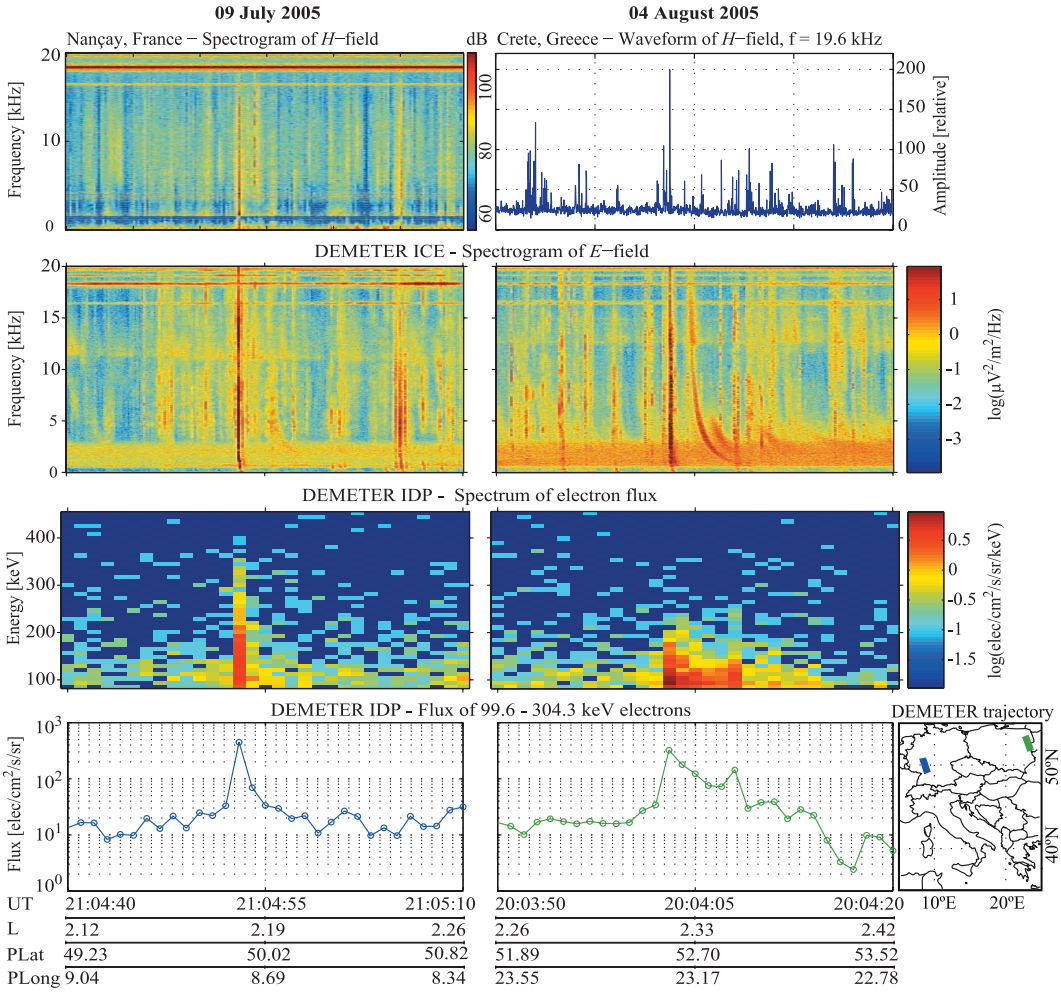

Figure 2. LEP bursts on DEMETER. (top to bottom) (left) Broadband VLF data and (right) narrowband VLF data from ground stations showing sferics caused by lightning strokes; spectrograms of electric field from ICE on DEMETER showing 0^+ whistlers from the same lightning strokes; electron spectra from IDP on DEMETER showing bursts of precipitated electrons; integral flux (99.6 to 304.3 keV). The map shows the trajectories of DEMETER satellite; blue and green respectively for the cases on the left and right.

Instrument (ICE) covering up to 20 kHz in burst mode, and the Instrument for Particle Detection (IDP) [*Sauvaud et al.*, 2006] measuring electrons from 72.9 keV to 2.35 MeV with 1 s resolution, and with a geometric factor of 1 cm^2 sr. IDP collimator views ~30° FWHM perpendicular to the orbit plane, measuring local pitch-angles near 90°.

[8] We also use VLF (up to 50 kHz) data from Stanford receivers in Nançay Astronomical Observatory, France (47°22′N, 2°11′E) and University of Crete, Greece (35°18′N, 25°04′E), and, when available, lightning location, timing and peak current data from the METEORAGE lightning detection network.

3. Observations

[9] DEMETER data were searched for LEP bursts in 309 burst mode passes over Europe (Figure 1) during July–September 2005, summer months with high lightning activity. Such LEP events were detected visually as short bursts of flux over a broad energy range [e.g., *Voss et al.*, 1998, Figure 4] in IDP data together with strong whistlers (upgoing 0^+ or once-reflected 1^-) in ICE data, two examples of which are shown in Figure 2. Burst of flux over a wide energy range is evident in IDP spectra and integral flux (99.6 to 304.6 keV) versus time. The 0^+ whistlers signify waves injected by lightning discharges, presumably leading to precipitation of electrons. VLF data from Nançay (9 July 2005) or narrowband data from Crete (4 August 2005) exhibit the temporal variation of nearby lightning activity. LEP bursts in IDP data are caused by singularly intense sferics (and hence lightning).

[10] Due to the 1 s resolution of IDP, the 0.4–0.6 s time delay (from causative lightning) is not measurable. This delay is expected from the travel time of whistlers to equatorial interaction regions and counter-streaming scattered electrons down to the ionosphere as observed in ground-based [e.g., *Peter and Inan*, 2004] and in S81-1/SEEP data [*Inan et al.*, 1989].

[11] Figure 3 shows LEP observations on 02 September 2005, also with METEORAGE lightning data (red dots). An active thunderstorm in Northwest Italy produces ~100 lightning discharges detected during this pass. As DEMETER moves northward towards the storm, number and intensity of 0^+ whistlers increase, while Nançay data show steady activity. A large region of enhanced particle flux is

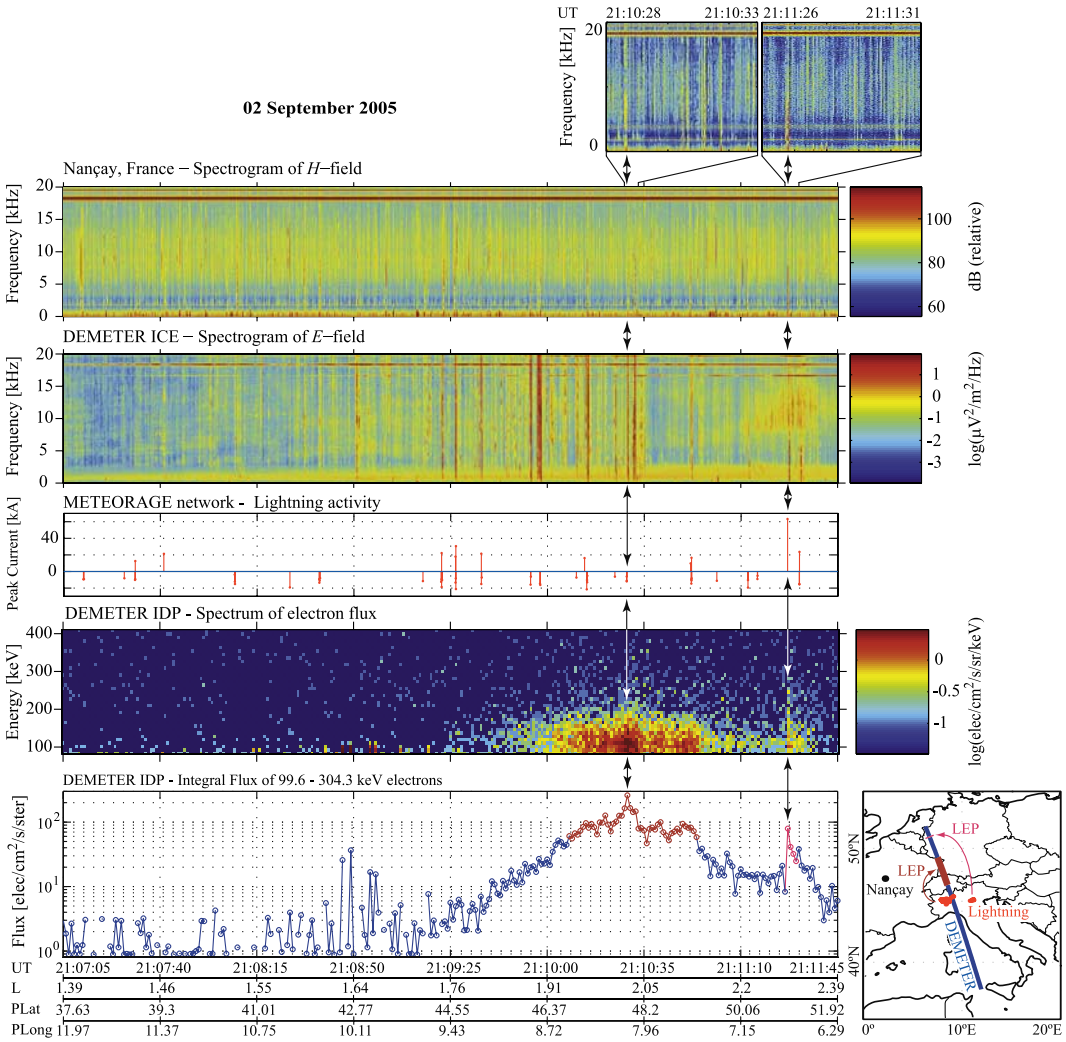

Figure 3. Region of enhanced precipitation flux produced by a thunderstorm and an individual LEP burst on 02 September 2005. (top to bottom) Spectrogram of magnetic field on the ground in Nançay, France; spectrogram of electric field from ICE on DEMETER; lightning activity as detected by METEORAGE network; electron spectra from IDP on DEMETER; integral flux (99.6 to 304.3 keV). The map shows DEMETER trajectory, with red dots representing lightning positions from METEORAGE network. As the satellite moves northward it enters the precipitation region with the particle detector measuring enhanced level of background flux during the portion of trajectory highlighted by brown color in the integral flux plot and on the map. At the end of the pass another stronger lightning to the east of the storm creates an individual LEP burst (highlighted by magenta color). The LEP burst at 21:11:26 UT (observed at the location pointed to with the red-arrow) is caused by a lightning flash in northern Italy.

observed slightly poleward of the storm, while 0^+ whistler activity starts and ends at lower latitudes (over the storm region). DEMETER first passes the injection region of whistler waves and subsequently the poleward-displaced precipitation region consistent with theoretical predictions [*Lauben et al.*, 2001, and references therein] and ground-based observations [*Peter and Inan*, 2004]. The peak value of integral flux coincides with triple negative lightning discharge indicated by the first sequence of arrows in Figure 3. A series of relatively intensive lightning also occurred around 21:09:25 UT and 21:11:10 UT, but any LEP bursts produced were not observed since DEMETER was then too far south or north respectively of the precipitation region (determined by the magnetospheric disposition of the whistler-mode raypaths [*Lauben et al.*, 2001]). The electron flux background levels before 21:09:25 UT represent levels typically observed during passes over Europe. The enhanced region of nearly two orders of magnitude higher precipitation flux underscores the contribution of LEP to radiation belt loss, being clearly the dominant loss driver in this region and for this particular thunderstorm.

[12] An individual LEP burst is observed at 21:11:26 UT in Figure 3, similar to those in Figure 2, simultaneously with an intense 0^+ whistler in ICE data and a sferic in Nançay data. METEORAGE specifies the causative lightning to be in Northern Italy (see map), while DEMETER was poleward.

[13] Out of 309 DEMETER passes analyzed, 22 LEP events were detected, shown in Figure 1 as red dots, all within $1.5 < L < 2.5$, varying from individual bursts (Figure 2) to regions with enhanced flux with sometimes one or more individual bursts discernible inside (Figure 3). Out of 22 LEP events, ~11 were detectable enhancements

of background flux (defined as regions of >10–15 s in duration), correlated with increased wave activity.

4. Discussion

[14] The upgoing 0^+ whistler in the 09 July 2005 case is not followed by a reflected 1^- component. For non-ducted propagation, whistler-mode raypaths are not field-aligned, and reflected components do not necessarily return to latitudes of injection. The upgoing 0^+ whistler on 04 August 2005 is followed by a 1^- whistler, which likely is simply a 1^- nonducted whistler, the raypaths for which did reach the satellite location. The endurance of the LEP burst for several seconds could be due to the atmospheric backscatter and mirroring of electrons [*Voss et al.*, 1998], but is not likely due to the 1^- whistler. LEP bursts with such extended tails were observed in other cases, with or without the presence of a 1^- whistler. The LEP burst on 02 September 2005 (Figure 3) is accompanied by a very weak 1^- whistler which may not be seen in Nançay due to the large distance to the lightning location, or simply due to the lack of whistler-mode ducts (necessary for observation on the ground [*Helliwell*, 1965, Figure 3–23]).

[15] DEMETER IDP electron energy spectra measured at high resolution (8.9 keV), shows general features for LEP events in Figures 2 and 3 basically consistent with that reported by *Voss et al.* [1998]; detailed comparison with theoretical model predictions is provided below. The LEP spectra on 04 August 2005 is typical and representative of the 22 cases of LEP events observed in DEMETER data.

[16] Figure 3 represents the first observation of enhanced (and most likely persistent) electron precipitation over a broad region maintained by a high rate of lightning flashes within a localized thunderstorm. Several individual LEP bursts, such as those in the middle of the region, are evident and are correlated in time with METEORAGE-recorded CG lightning. METEORAGE does not record intra-cloud (IC) lightning discharges which undoubtedly also occur, and which can also launch whistler-mode waves into the lower ionosphere directly overhead, and may thus also contribute to the creation and maintenance of this enhanced continuum of precipitation. Precipitation due to magnetospherically reflected whistlers (typically reflecting well above 700 km, i.e., not observable on DEMETER) may also contribute to enduring precipitation over large regions [*Bortnik et al.*, 2006]. This observation indicates that the role of the LEP process may have heretofore been underestimated, at least in terms of the total regional effect of individual thunderstorms. While wide LEP enhancement regions were not identified in the S81-1/SEEP data, they may simply not have been recognized due to lack of lightning and whistler data. Such effects would have been naturally overlooked in ground-based subionospheric VLF observations, relying on detection of transient burst effects.

5. Theoretical Model Analysis

[17] We use a model of lightning-generated whistler-induced electron precipitation [*Bortnik et al.*, 2006] to calculate the expected precipitation signatures for an individual LEP burst observed on DEMETER (Figure 3). The identification of the causative lightning discharge by a lightning detection network allows for the first time to compare the direct satellite observations with the model. The lightning location (11.15°E, 45.46°N), time (21:11:26.84 UT), and peak current (+63.30 kA) are used as inputs, while lightning spectrum is modeled after *Uman* [1984, p. 61], with parameters set to match the spectrum observed at Nançay for the causative lightning-associated sferic. Magnetospheric whistler propagation is simulated using the Stanford VLF ray tracing code [*Inan and Bell*, 1977], including Landau damping effects [*Bortnik et al.*, 2006]. The cold plasma density is based on work by *Tarcsai et al.* [1988], while the trapped electron populations (with a 'sinusoidal' pitch angle distribution) are based on AE-8 radiation belt model [*Vette*, 1991]. The calculation [*Bortnik et al.*, 2006] yields precipitated flux as a function of energy, *L*-shell, longitude, and time. The resultant flux is essentially proportional to the trapped flux at the edge of the loss cone [*Inan et al.*, 1989] and is also dependent on the energy spectra of the trapped population. Given that independent data on the trapped flux is not available, starting with an assumed trapped electron distribution would likely lead to expected differences between model and observations.

[18] Figure 4a shows a map of the DEMETER pass with model-calculated precipitated number flux (100–300 keV) superimposed. The poleward displacement of the precipitation region with respect to the causative lightning is consistent with past observations [*Peter and Inan*, 2004], and the modeled location of the precipitation agrees with that of DEMETER at the time of observation. The satellite does not observe this particular event at the calculated location of peak precipitation (simply because the orbit does not go through the region of the peak); instead at the time of the LEP burst, DEMETER is located ~200 km west of the peak. The left and right panels of Figure 4b respectively show the calculated precipitated differential number flux at the satellite location and that observed on DEMETER, a four-second snapshot of the data shown in Figure 3. Note the different scales (marked on the left and right sides of the color bar). Time zero indicates the time of the causative lightning flash. The onset delay between the lightning and the onset of precipitation as calculated by the model is consistent with the timing of precipitation observed on DEMETER. Figure 4c shows the precipitated energy spectra observed on DEMETER (taken in the range $0.16\ \text{s} < t < 1.16\ \text{s}$) and that calculated by the model (shown on different scales). DEMETER data >300 keV are not shown due to the low detector counts. The difference in scale between the calculated and observed precipitation indicates that the number of particles near the loss-cone-edge may have been higher at the time of the LEP event than that used in the model (i.e., the initial pitch angle distribution was 'harder' than the 'sinusoidal' one used). The differences in the shape of the energy spectra could well be due to the fact that the trapped electron spectra was different than the AE-8 model used here. In general, however, both the data and model are consistent with electron energies of ~100–300 keV being involved, and the fact that the LEP burst arrives within <1 s of the causative lightning discharge.

6. Summary

[19] The data presented herein constitute the first simultaneous measurements of both the causative whistlers and

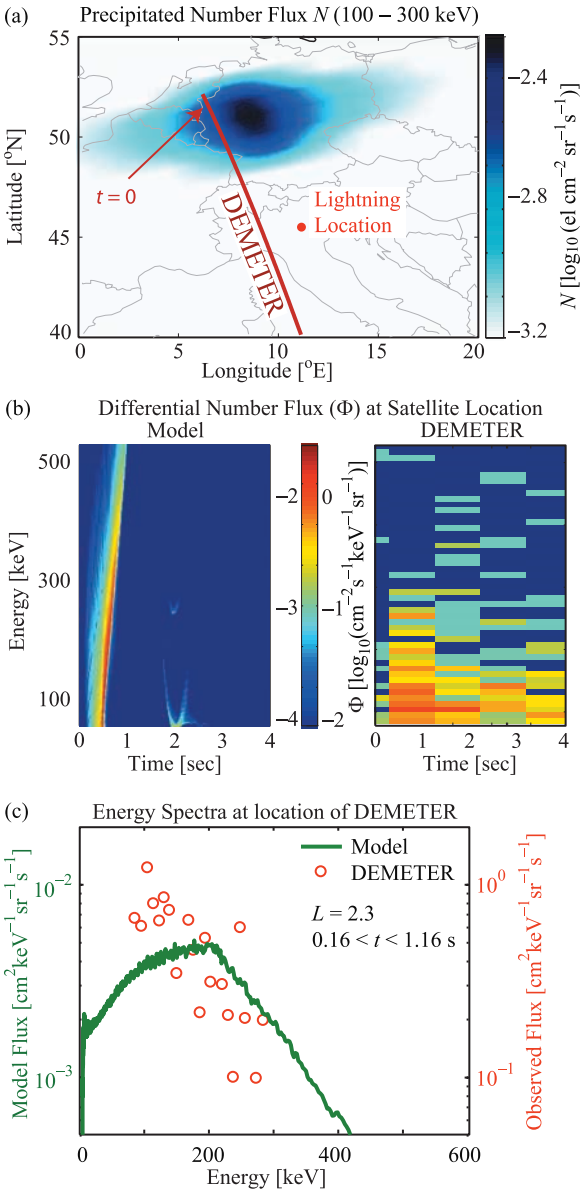

Figure 4. Comparison of DEMETER observations to predictions of a theoretical model of whistler-induced electron precipitation. (a) Map of the DEMETER pass, with modeled precipitated number flux (100–300 keV) superimposed. The location of the causative lightning (45.46°N, 11.15°E) and the satellite (50.96°N, 6.75°E) at the time of detection is shown. (b) Differential number flux at the location of DEMETER at the time of detection, (left) calculated by the model and (right) observed on DEMETER. Time zero is the time of the causative lightning flash (21:11:26.84 UT). (c) Comparison of the observed (shown in red) and the modeled (shown in green) precipitation energy spectra.

scattered energetic electrons on the same spacecraft, and further reveals the presence of large regions of enhanced precipitation apparently maintained by the totality of lightning activity in localized thunderstorms. The LEP bursts and enhancements consist of electrons with 100–300 keV energy, arriving within <1 s of the upgoing whistler waves injected by the causative lightning discharges which are geo-located for some satellite LEP events. Our results should allow better quantification of the role of the LEP process in the loss of electrons from the radiation belts.

[20] **Acknowledgments.** The Stanford portion of this work was supported by the Defense Advanced Research Projects Agency (DARPA) and the High Frequency Active Auroral Research Program (HAARP) under ONR grants N00014-06-1-1036 and N00014-03-1–0630 to Stanford University. We thank METEORAGE for the provision of lightning data and T. F. Bell for his useful comments.

References

Abel, B., and R. M. Thorne (1998), Electron scattering loss in Earth's inner magnetosphere: 1. Dominant physical processes, *J. Geophys. Res.*, *103*, 2385–2396.

Bortnik, J., U. S. Inan, and T. F. Bell (2006), Temporal signatures of radiation belt electron precipitation induced by lightning-generated MR whistler waves: 1. Methodology, *J. Geophys. Res.*, *111*, A02204, doi:10.1029/2005JA011182.

Clilverd, M. A., C. J. Rodger, and D. Nunn (2004), Radiation belt electron precipitation fluxes associated with lightning, *J. Geophys. Res.*, *109*, A12208, doi:10.1029/2004JA010644.

Helliwell, R. A. (1965), *Whistlers and Related Ionospheric Phenomena*, Stanford Univ. Press, Stanford, Calif.

Helliwell, R. A., J. P. Katsufrakis, and M. L. Trimpi (1973), Whistler-induced amplitude perturbation in VLF propagation, *J. Geophys. Res.*, *78*, 4679–4688.

Imhof, W. L., J. B. Reagan, H. D. Voss, E. E. Gaines, D. W. Datlowe, J. Mobilia, R. A. Helliwell, U. S. Inan, J. P. Katsufrakis, and R. G. Joiner (1983), The modulated precipitation of radiation belt electrons by controlled signals from VLF transmitters, *Geophys. Res. Lett.*, *10*, 615–618.

Inan, U. S., and T. F. Bell (1977), The plasmapause as a VLF wave guide, *J. Geophys. Res.*, *83*, 2819–2827.

Inan, U. S., H. C. Chang, R. A. Helliwell, W. L. Imhof, J. B. Reagan, and M. Walt (1985), Precipitation of radiation belt electrons by man-made waves—A comparison between theory and measurement, *J. Geophys. Res.*, *90*, 359–369.

Inan, U. S., M. Walt, H. Voss, and W. Imhof (1989), Energy spectra and pitch angle distribution of lightning-induced electron precipitation: Analysis of an event observed on the S81-1 (SEEP) satellite, *J. Geophys. Res.*, *94*, 1379–1401.

Lauben, D. S., U. S. Inan, and T. F. Bell (2001), Precipitation of radiation belt electrons induced by obliquely propagating lightning-generated whistlers, *J. Geophys. Res.*, *106*, 29,745–29,770.

Parrot, M. (Ed.) (2006), Special issue: First results of the DEMETER micro-satellite, *Planet. Space Sci.*, *54*(5), 411–558.

Peter, W. B., and U. S. Inan (2004), On the occurrence and spatial extent of electron precipitation induced by oblique nonducted whistler waves, *J. Geophys. Res.*, *109*, A12215, doi:10.1029/2004JA010412.

Sauvaud, J. A., T. Moreau, R. Maggiolo, J. P. Treilhou, C. Jacquey, A. Cros, J. Coutelier, J. Rouzaud, E. Penou, and M. Gangloff (2006), High energy electron detection onboard DEMETER: The IDP spectrometer, description and first results on the inner belt, *Planet. Space Sci.*, *54*(5), 502–511, doi:10.1016/j.pss.2005.10.019.

Tarcsai, G., P. Szemeredy, and L. Hegymegi (1988), Average electron density profiles in the plasmasphere between L = 1.4 and 3.2 deduced from whistlers, *J. Atmos. Terr. Phys.*, *50*, 607–611.

Uman, M. A. (1984), *Lightning*, Dover, Mineola, N. Y.

Vette, J. (1991), The AE-8 trapped electron model environment, *Rep. 91-24*, Natl. Space Sci. Data Cent., Greenbelt, Md.

Voss, H. D., et al. (1984), Lightning-induced electron precipitation, *Nature*, *312*, 740–742, doi:10.1038/312740a0.

Voss, H. D., M. Walt, W. L. Imhof, J. Mobilia, and U. S. Inan (1998), Satellite observations of lightning-induced electron precipitation, *J. Geophys. Res.*, *103*, 11,725–11,744.

U. S. Inan, W. B. Peter, and D. Piddyachiy, STAR Laboratory, Stanford University, Packard Bldg. Rm. 355, 350 Serra Mall, Stanford, CA 94305, USA. (inan@stanford.edu)

M. Parrot, Laboratoire de Physique et Chimie de l'Environnement, CNRS, 3A Avenue de la Recherche Scientifique, F-45071 Orléans cedex 2, France.

J. A. Sauvaud, Centre d'Etude Spatiale des Rayonnements, CNRS, 9 avenue du Colonel Roche, BP 4346, F-31028 Toulouse cedex 4, France.